Optimum Performance of UHF RFID Tags in Dielectric Environment

Lakshmi Anusha Kosuru

Submitted to the graduate degree program in Electrical Engineering & Computer Science and the Graduate Faculty of the University of Kansas School of Engineering in partial fulfillment of the requirements for the degree of Master of Science

Thesis Committee:

Dr. Daniel D. Deavours: Chairperson

Dr. Kenneth Demarest

Dr. Sarah Seguin

Date Defended

The Thesis Committee for Lakshmi Anusha Kosuru certifies
that this is the approved version of the following thesis:

Optimum Performance of UHF RFID Tags in Dielectric Environment

Committee:

_____

Chairperson

_____

_____

_____

Date Approved

Abstract

Ultra High Frequency Radio Frequency Identification (UHF RFID) technology has gained prominence in recent years. It is being deployed extensively in supply chain and asset tracking by retailers to better control their inventory. The main drawback of UHF RFID tag antenna is that it is sensitive to the environment in which it operates. The performance of the tag degrades when placed on conductive or dielectric objects. While RFID tags near metal have been extensively evaluated in the literature, tags on and in dielectric media have received less scrutiny and rigorous evaluation. In this thesis, we develop a rigorous theoretical model for the behavior of RFID tags immersed in a dielectric medium using the Uda model and embedded T-match antenna. From this, we are able to investigate a number of criteria for optimality. We find that the simplest optimality condition is not physically realizable, and more realizable models yield several results that are of practical interest. Also, we propose a method to determine the input impedance of a center-fed dipole using a five element equivalent circuit. We relax the conditions for optimality and do an exhaustive search for the optimal design over the parametric space. Finally, we validate the model and present the trade-off to be made with the power transfer efficiency to obtain a tag working in wider range of dielectric materials. We make two specific recommendations for future work to increase the accuracy and usefulness of this work.

To my family

Acknowledgements

I am highly indebted to my advisor, Dr.Dan Deavours, for his invaluable guidance and constant support. Without his help and expert advice, none of this would have been possible. I also wish to thank him for encouraging me to aim higher and for motivating me to do high quality work. I am grateful to my mentor and great teacher, Prof.Ken Demarest, for teaching me the basics of electromagnetics, for his invaluable inputs to my thesis work and for being my source of inspiration. I also would like to thank Dr.Sarah Seguin for being on my committee and reviewing my thesis.

Special thanks go to my good friend and colleague, Naaser Mohammed, for extending help and support through the course of my thesis work. I wish to thank all my friends here at KU for being part of the most cherished two years of my life. Last but not the least, I owe my deepest gratitude to my parents and love for my brother for making me the person I am today and for always being there for me.

Contents

List of Figures

List of Tables

Chapter 1

Introduction and Motivation

Radio Frequency Identification (RFID) is a tracking technology used to identify objects using radio communications [1]. A RFID system consists of a reader that transmits radio signals via an antenna connected to it, and a tag that backscatters the modulated signal with tag ID information. The RFID tag has an integrated circuit (chip) and a antenna.

The frequency bands used in RFID technology are low-frequency (LF), 125–134 kHz, high-frequency (HF) 13.56 MHz, ultra-high-frequency (UHF) 860–960 MHz and microwave 2.4–2.45 GHz. LF and HF operation involves inductive coupling and so the tags use coils as antennas. The disadvantages of the LF and HF RFID system is that the read range of the tags is limited by the size of the antenna and the manufacturing cost of the coil antennas is relatively high. For UHF and microwave frequency range, the operation is through radiative coupling and the tag designs use dipole variants as antennas. The UHF and microwave frequency tags provide long read distances, and as the antennas have simple planar structures, they can be manufactured using the inexpensive printed conductor technology. However, the tags for microwave frequencies have shorter read range

than the UHF tags (1–3 m at 2.4 GHz vs 2–10 m at 900 MHz). Therefore, the UHF RFID tags are being extensively deployed in asset tracking and supply chain management as they are small in size, achieve read ranges of several meters, support high data rates, and are available at low cost.

The RFID tags can be further classified by the presence or absence of a power source and a radio transmitter into three types: passive, semipassive, and active tags. Passive tags do not have an independent power source and rely on backscattered communications for the tag-to-reader communication usually referred to as *up-link*. Semipassive tags have a local battery that powers the chip and backscattering is used for up-link communications. The active tags, in addition to a battery to power the chip, have a conventional transmitter for the up-link communications. Thus, passive tags are simple and inexpensive, but their read range is limited by the transmit power. In order to increase the read range of the passive RFID tag, the tag antenna needs to be designed so that maximum power can be transfered to the chip. The input impedance of the chip used in a passive UHF RFID tag is generally capacitive, and in order to have maximum power transfer, the tag antenna's impedance needs to transformed to be inductive. Typically, it is done by using matching networks like T-match and Inductively coupled loop [1].

Most of the commercially available UHF tag antenna designs use variants of a folded dipole and are designed for a specific environment such as air, metal, paperboard, plastics like polyvinyl chloride (PVC) etc [2]. The major technical drawback of a UHF antenna is its sensitivity to the material on which the tag is placed. The materials can be broadly categorized into conductors and dielectrics like PVC. To make the UHF RFID technology economically viable, it is essential that a tag be used while attached to a variety of objects. While RFID in metallic

environments have received much attention recently [3], there has been relatively little rigorous work examining how tags interact with dielectric media. In this thesis, we lay a rigorous, theoretical foundation for RFID tag performance on dielectric materials, including practical bounds on what is possible.

Figure 1.1. Commericial products tagged using UHF RFID.

Retailers have been using UHF RFID tags to track pallets of merchandise traveling through their supply chains to better control their inventory. Thus, the UHF RFID tags need to work effectively in complex dielectric environments like some of the commercial products shown in Figure. 1.1. For example, a tag can be placed on a "cardboard" (corrugated fiberboard) box, with contents in the box having various air spacings, additional packaging, and otherwise a complex heterogeneous dielectric environment. It is well known that the performance of the UHF RFID antenna degrades when placed on a dielectric material. Therefore, it is important to analyze, understand, predict, and optimize RFID tags for these environments. It is a common approach to transform a complex heterogeneous dielectric environment into an equivalent homogeneous dielectric environment, and then perform the analysis. In this thesis, we rigourously analyze and optimize the antenna for a

lossless homogenous environment and deduce conclusions that could be insightful and lead to useful work for heterogenous environments. In particular, we answer the following questions that arise when a antenna is immersed in homogeneous dielectric medium:

- Can we achieve an antenna design that is "perfectly matched" in homogenous media with different relative permittivity?
- If not, for a given form factor of the antenna, how well can we match the antenna such that it could be immersed in a specified range of dielectric media?
- How much "dielectric bandwidth" can be achieved from the antenna of fixed form factor for a specific power transfer efficiency τ_{min}?

For this, we theoretically model the scenario in which RFID tag is placed on heterogeneous dielectric enviroment as "tag on slab". In this model, the tag is considered to be placed at the interface of two semi-infinite spaces i.e., half the space is filled with air and the other half space is dielectric medium of relative permittivity ϵ_r. This model is then transformed into a medium filled with homogeneous dielectric of effective relative permittivity ϵ_{eff}. The rest of the analysis is then conducted on a RFID antenna immersed in dielectric medium. In particular, we use "Embedded-T" introduced by Mohammed et al. [4], which is a simple structure that has been rigorously analyzed using the Uda circuit model. The classic Uda model addresses the input impedance of a T-match generally as a function of frequency. It is well known that wavelength of a plane wave changes either with the change in frequency of the wave or when the relative permittivity of the medium changes. Based on this analogy between the frequency and dielec-

tric domains, we introduce "immersion Uda model" for the T-match antenna in homogenous dielectric environment. This model is analyzed to obtain optimality condition for the antenna in dielectric environments. Ideally, the "optimal" antenna is perfectly matched in air and unperturbed by small changes in the permittivity of the environment. This analysis yields a condition that is numerically amenable but practically impossible to satisfy. To improve accuracy of the model, an equivalent circuit useful for computation of the input impedance of center-fed ribbon dipole is also presented. We introduce a new term "dielectric-bandwidth" and propose a numerical method, based on brute-force search, to obtain a robust tag antenna for a given power transfer effciency coefficient τ_{min}. The simulations for validation are done in High Frequency Structure Simulator (HFSS), a industry-standard simulation tool for $3D$ full-wave electromagnetic field simulation. We observe that the experimental results concur with the predictions of the model and conclude that the analysis of the model is accurate.

The rest of the thesis is organized as follows. The required background theory of RFID antenna design, T-match and its analysis using Uda model, design equations for a planar folded dipole, as well as other related works in this subject area are discussed in Chapter 2. In Chapter 3, the "tag on slab" model is explained, and the frequency-dielectric transformation on the input impedance of the T-match in the "immersed Uda model" is derived. The analytic and numerical approach using the improved equivalent circuit for common mode impedance to solve for the "optimal" antenna is presented in Chapter 4. Performance results of the optimized antenna design are shown in Chapter 5. The evaluation of the results, limitations of the theoretical model, and the future work to be done on the heterogenous environments is discussed in Chapter 6.

Chapter 2

Background and Related Work

In this chapter, description for the concepts that were introduced in Chapter 1 are provided. In Section. 2.1, the basics of passive UHF RFID system are given. The term *power transfer efficieny* τ, which is an important performance metric for RFID tag antenna design, is defined. The Uda analysis for a wire dipole T-match antenna is briefly outlined and the design equations applicable to coplanar folded dipole are provided in Section. 2.2. Next, we outline the advantages of the "embedded-T" introduced by Mohammed et al. [4]. The literature related to the analysis and synthesis of UHF RFID tags in dielectric environments is reviewed in Section. 2.4

2.1 Passive UHF RFID System

An RFID system consists of an interrogator sometimes called reader and a transponder or tag. A host computer is connected to the reader to control the operation of the reader, and to store and display the resulting data. The block diagram of a RFID system is shown in Figure. 2.1 [1].

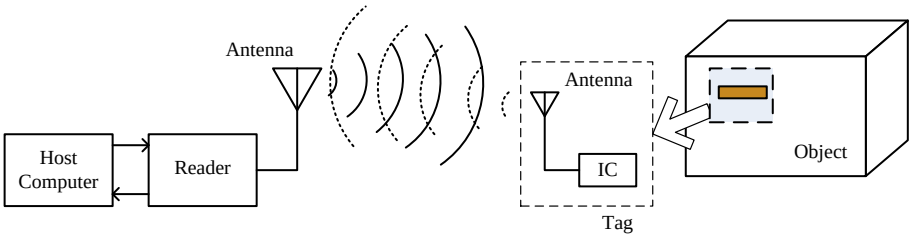

Figure 2.1. Overview of a Passive RFID System

The reader is generally integrated with either a monostatic or bistatic 6 dBi patch antenna. This antenna is used to transmit radio waves when the reader is prompted by the host computer. This transmission of data is generally known as the *down-link* and is used to request the tag to send information back to the reader. The tag contains an antenna attached to the chip, which contains the tag ID and the digital logic needed for communication. Once the carrier signal reaches the RFID tag, the RFID chip is powered. The received signal is modulated with the tag ID before it is backscattered by the tag antenna to the reader. This channel carrying data from tag to reader is known as the *up-link*. The data received by the reader's receiver antenna is decoded by the reader and transmitted to the host antenna for further processing.

The UHF frequency range is 860 to 960 MHz and its operation provides range that is limited by transmit power. The UHF tags use simple dipole like antennas that are easily fabricated, but size is constrained due to wavelength of the radiation. Passive UHF RFID tags have no independent power source to drive the circuit. The received power is rectified to power the circuitry in the attached chip and then backscattered after modulation. To maximize the tag performance, the power available at the tag antenna should be efficiently delivered to the chip.

According to the maximum power transform theorem, the power, from the

source (antenna), delivered to the load (chip), is maximum when the source impedance is complex conjugate of the load impedance. In the case of RFID tags, the antenna impedance must be matched to complex impedance of the chip unlike the traditional antennas like cylinderical dipoles, which are matched to resistive loads of 50 Ω or 75 Ω. For maximum power transfer, the input impedance of the antenna Z_{in} should be complex conjugate of the chip impedance i.e., $Z_{in} = Z_{ic}^{*}$, where Z_{ic} is the IC impedance. Nikitin et al. [5] reviewed the power reflection coefficient for RFID tags. For an antenna with input impedance $Z_{in} = R_{in} + jX_{in}$ with a chip placed at its input terminals, *power transfer coefficient* τ can be expressed as follows [1]

$$\tau = \frac{4R_{in}R_{ic}}{\mid Z_{in} + Z_{ic} \mid^2} \tag{2.1}$$

where $Z_{ic} = R_{ic} + jX_{ic}$ is the chip impedance

The chip impedance, in a UHF RFID tag, has large capactive reactance. We know that simple half wave dipole has small reactance and so the power transfer efficieny will be low in this case. Also, size (form factor) of the tag is a constraint in UHF RFID applications and so a dipole of 16 cm is too big for labels. Therefore, we need to transform the impedance of a simple short dipole to match it to the UHF RFID chip. Some of the common methods for size reduction are meandering, capacitive tip-loading and inverted F configurations. For conjugate impedance matching, structures like T-match, inductively coupled loops and nested slots are used [6].

2.2 The Uda Model

Most commonly used matching structure is the T-match. It is a simple, augmented dipole that is used to scale the dipole impedance and provide a shunt (typically inductive) reactance. The T-match is discussed at length in numerous texts such as [7] and a survey in [6]. Uda [8], analyzed the T-match and proposed a model to compute its input impedance. In this section, we briefly review the classic Uda model for wire dipoles in Section. 2.2.1 and then present the design equations for the model parameters for a strip dipole in Section 2.2.2.

2.2.1 Classic Uda Model

The T-match consists of two dipoles connected as shown in Figure. 2.2 [7]. The smaller dipole of radius a' and length l' is tapped to the second dipole of length l and radius a at a distance of $l'/2$ from the center. The voltage source is connected to the center of arm-1 with the smaller dipole of length l'.

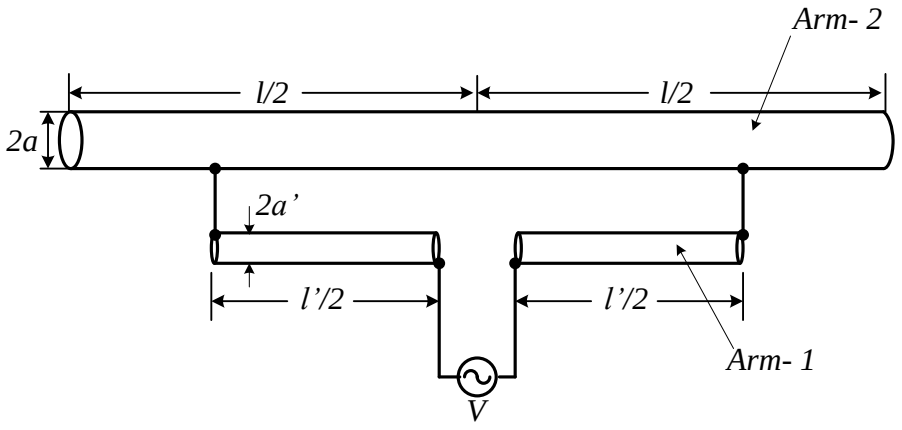

Figure 2.2. T-match antenna

In Uda's analysis, the antenna response is considered to be sum of its radiating

and non-radiating components shown in Figure. 2.3. For this, even-odd mode analysis is done. A *faux* voltage source is inserted at the center of arm-2 with the larger dipole and the structure is driven in common and differential modes. In

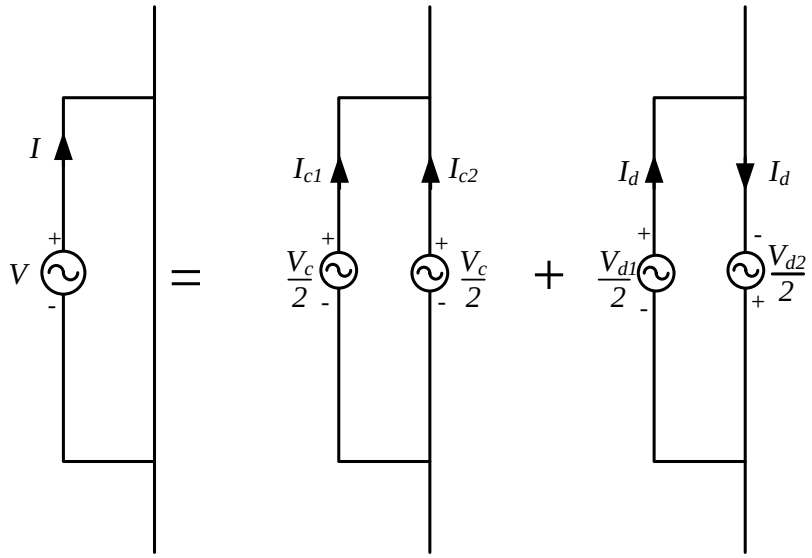

Figure 2.3. Radiating and non-radiating components

the common-mode, the voltage source in arm-1 (V_{c1}) and arm-2 (V_{c2}) are equal in amplitude and phase. The current in the arm-1, I_{c1}, and current in arm-2, I_{c2}, are in the ratio $1 : \alpha$, where α is called the *splitting factor*. I.e.,

$$V_{c1} = V_{c2},$$

$$\frac{I_{c2}}{I_{c1}} = \alpha.$$

In differential mode, the source voltages in the two arms (V_{d1} and V_{d2}) are set in the ratio of splitting factor α. The currents in the two arms (I_{d1} and I_{d2}) are

equal in amplitude but 180^0 out of phase. I.e.,

$$\frac{V_{d2}}{V_{d1}} = -\alpha,$$

$$I_{d1} = -I_{d2}.$$

The T-match is also modeled by antenna (common mode) and transmission line (differential) modes. The common mode impedance, Z_c, is input impedance of a center fed dipole. Self-impedance solutions to compute the input impedance of center fed cylinderical dipoles exist [7].

The differential mode impedance, Z_d, is that of a shorted transmission line of length $l'/2$, constituted by the two dipoles (as shown in Fig. 2.4), [8] i.e.,

$$Z_d = j2Z_0 \tan\frac{\beta l'}{2}\,. \tag{2.2}$$

where β is the propagation constant of the medium and Z_0 is the characteristic impedance of the two-conductor transmission line.

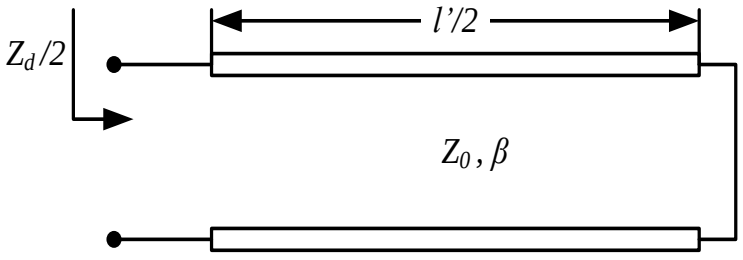

Figure 2.4. Shorted Transmission line

The "splitting factor" α acts as an impedance multiplier of the common mode. The three terms Z_c, Z_d, and α are combined to produce the input impedance, Z_{in},

according to the following expression [8]

$$Z_{in} = \frac{(1+\alpha)^2 Z_c Z_d}{(1+\alpha)^2 Z_c + Z_d} \tag{2.3}$$

The equivalent circuit model representing the T-match antenna is shown in Figure. 2.5.

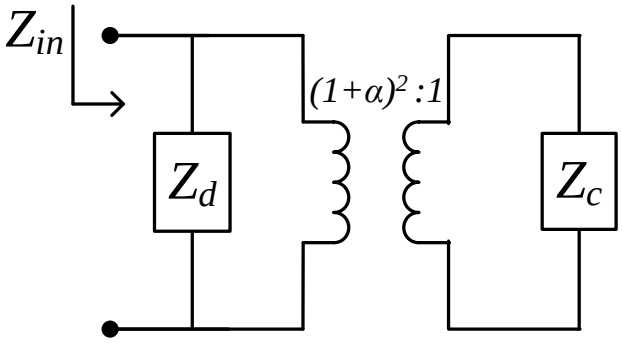

Figure 2.5. Uda circuit model of T-match

For simplicity, we sometimes use the *antenna impedance*, Z_a, which is given as,

$$Z_a = (1+\alpha)^2 Z_c, \tag{2.4}$$

which is the scaled common mode impedance. I.e., $R_a = (1+\alpha)^2 R_c$ and $X_a = (1+\alpha)^2 X_c$

2.2.2 Strip Dipole Uda Model

In general, the commercial RFID tags are planar dipoles because they can be easily manufactured using the inexpensive printed conductor technology. A planar folded dipole constructed using asymmetric coplanar strips is shown in Figure. 2.6 [9]. The strip S_1 of width W_1 and strip S_2 of width W_2 form the two

arms of the folded dipole and the two strips are separated by a distance of M. The length of the slot is S. The strip S_1 is the driven strip. Lampe in [9,10] applied the classic Uda model to a Coplanar Strip (CPS) folded dipole antenna and proposed new design equations for the splitting factor α and the characteristic impedance Z_0 of the transmission line in differential mode. Note that one of the major assumptions in [9] is that the medium surrounding the antenna is homogenous. In this section, we discuss methods and design equations for Uda model parameters Z_c, Z_d and α applicable to planar folded dipole topologies.

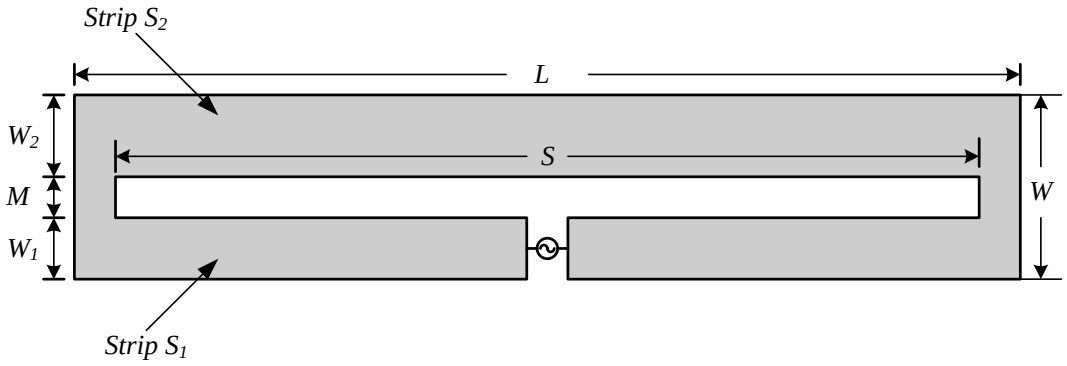

Figure 2.6. Coplanar Folded Dipole

First, let us consider the method to compute common mode impedance, Z_c. As we know, it is input impedance of a center-fed ribbon dipole of length L and width W. For a thin strip with $\beta W << L$ and $W << L$, Z_c can be computed from an equivalent cylindrical dipole of radius a and length l using the relationship between a and W as $a = W/4$. Most of the commercial RFID tag antennas do not meet the upper limit of the conditions $\beta W << L$ and $W << L$. Moreover, the RFID tag antennas are meandered making the application of the self-impedance solutions improbable. Therefore, in this thesis, we propose a equivalent circuit

model (explained in detail in Chapter 4), which is dependent on the Finite Element Method FEM tool to compute Z_c.

Next, consider the differential mode impedance, Z_d. It is twice the input impedance looking into a shorted transmission line of length $S/2$. Here S is the length of the slot. Thus, (2.2) can be re-written in terms of slot length S as,

$$Z_d = j2Z_0 \tan\frac{\beta S}{2}. \tag{2.5}$$

The term Z_0, in this case, is the characteristic impedance of a coplanar strip transmission line. For a CPS in a homogenous medium, Z_0 is given by (2.6) [9,10]

$$Z_0 = \frac{120\pi}{\sqrt{\epsilon_r}}\frac{K(k)}{K'(k)}, \tag{2.6}$$

where $K(k)$ is complete elliptic function of first kind, $K'(k) = K(k')$ and $k'^2 = 1 - k^2$. For asymmetrical strips, i.e., $W_1 \neq W_2$, k is given as

$$k = \frac{M/2[1 + e(M/2 + W_1)]}{M/2 + W_1 + e(M/2)^2}, \tag{2.7}$$

$$e = \frac{W_1W_2 + M/2(W_1 + W_2) - [W_1W_2(M + W_1)(M + W_2)]^{1/2}}{(M/2)^2(W_1 - W_2)}. \tag{2.8}$$

If the strips are symmetrical, i.e., $W_1 = W_2$, then the parameter k reduces to $k = \frac{M}{M+2W_1}$. For planar folded dipole antennas realized on finite dielectric slab, improved design equations for Z_0 exist [11,12].

Now, consider the splitting factor, α. In the common mode, α is the ratio of the current on strip S_2 and the current on the strip S_1. For a planar folded dipole, the current in common mode divides between the two conducting strips S_1 and S_2 with respect to the ratio of charges accumulated on the two strips when both

the strips are excited by the same potential [9, 10]. The ratio of currents that is equal to the ratio of charge distributions on the two conducting strips is found by solving the two-dimensional asymmetric coplanar strip problem. The final form for α is given by (2.9) [9, 10]

$$\alpha = \frac{ln\left(4c + 2\left[(2c)^2 - (W_1/2)^2\right]^{1/2}\right) - ln\,(W_1)^2}{ln\left(4c + 2\left[(2c)^2 - (W_2/2)^2\right]^{1/2}\right) - ln\,(W_2)^2}, \tag{2.9}$$

where W_1 and W_2 are the widths of the coplanar strips and M is the distance between the strips and $c = (\frac{(W_1+W_2+2M)}{4})$

The equations (2.5), (2.6), (2.9) and (2.3) constitute the *strip dipole Uda Model*.

2.3 Embedded T-Match

In this thesis, we use the "embedded-T" introduced by Mohammed et al. [4]. The *Embedded T* antenna, shown in Fig. 5.2, is a rectangular planar dipole of length L and width W ($W = W_1 + W_2 + M$) with the T-match embedded into the structure itself. The other parameters of this structure are slot length S, gap M and widths W_1 and W_2.

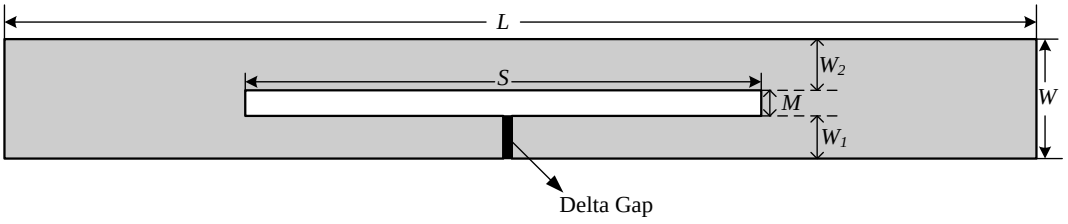

Figure 2.7. An example "embedded-T" antenna.

In particular, we are using the embedded-T match antenna as it has the following advantages over the other commonly used antenna structures [4]:

- The structure is simple.
- It has only four independent parameters (L, W, W_1, S).
- The Uda model can be applied to the structure.
- The closed form expressions for Z_0 (2.6) and α (2.9) exist.

Now that we have covered the basic concepts of the passive RFID antenna design and analysis of T-match antenna using Uda model, we review the literature related to the analysis and synthesis of antenna design in dielectric environments in the next section.

2.4 Literature Review

The traditional antennas, like dipoles, have been rigourously analyzed in dielectric environments [13, 14]. As stated earlier, the RFID antennas are different from the traditional antennas. The RFID antennas are generally planar structures constrained by size and cost, and need to incorporate matching structures to match to a complex load.

When tags are placed on dielectric mediums, the performance is degraded as the antenna is de-tuned and significanlty less work has been published on this effect. Early studies showed empirical results for existing antenna designs when placed on different objects like metal or dielectrics [15, 16]. In [15], various types of tags are tested when placed on dielectrics/metals for quantitative analysis of

different designs. Griffin et al., [16], propose new terms like *gain penalty* to quantify the reduction in RF tag antenna gain due to material attachment. In [17], a novel antenna design using series and shunt stubs for matching is proposed for paper based UHF RFID tags. The variation of input impedance of the antenna is studied only over the required dielectric range of 3.2 to 4 to optimize the antenna design. Some works like [2, 18], employ genetic algorithms with simulation tools like IE3D of Zealand EM simulators,Ansoft Designer respectively, to find robust antenna designs to work over a large range of dielectrics. These solutions are effective for point solutions, but are less useful for developing a rigorous analysis. Deleruyelle et al. [19] proposes a broadband antenna based on the Vivaldi antenna as a potential solution for dielectrics and measured the orthogonal gain and read range as function of the material's relative permittivity and thickness. The Vivaldi antenna is impractical for RFID applications due to its size. Some have investigated dipole-based RFID antenna designs, such as Choo et al. [20], which uses an inductively coupled loop to improve insensitivity to dielectrics. The optimization of the loop structure and the antenna geometry is done based on the calculated maximum read distance. Manzi and Feliziani [21] study the effect of the UHF RFID IC impedance on the performance and show that the quality factor Q of the chip is a dominant factor in dielectric-sensitivity. Finally, Choo et al. [22] show a preferred antenna for placement on thin dielectric materials and offers an explanation based on the stability of the matching circuit. Our effort seeks to build on these prior works by constructing a more holistic analysis, including both the antenna and matching network.

In brief, we described a passive UHF RFID system, defined power transfer efficieny for a RFID tag and reviewed Uda model for T-match antennas in this

chapter. In the next chapter, we utilize the Uda model and embedded T-match antenna to propose and validate a theoretical model for a RFID antenna immersed in dielectric environments.

Chapter 3

Theoretical Model

In this chapter, we develop a theoretical model to analyze RFID tags in homogenous dielectric environments. We consider a typical RFID application where the tag is placed on a cardboard box filled with different materials. This scenario is modeled as "tag on slab" in Section 3.1. We derive the effective dielectric constant for homogenous medium that maps to the dielectric constant of the slab in "tag on slab" scenario. In Section 3.2, we present the "immersed Uda model" for an antenna immersed in a lossless homogeneous medium based on the frequency- dielectric transformation. We validate the "immersed Uda model" in Section. 3.2.1.

3.1 Tag on Slab Model

Consider a tag placed on a large "cardboard" (corrugated fiberboard) box, with contents in the box having various air spacings, additional packaging, and otherwise a complex heterogeneous dielectric environment as shown in Figure. 3.1.

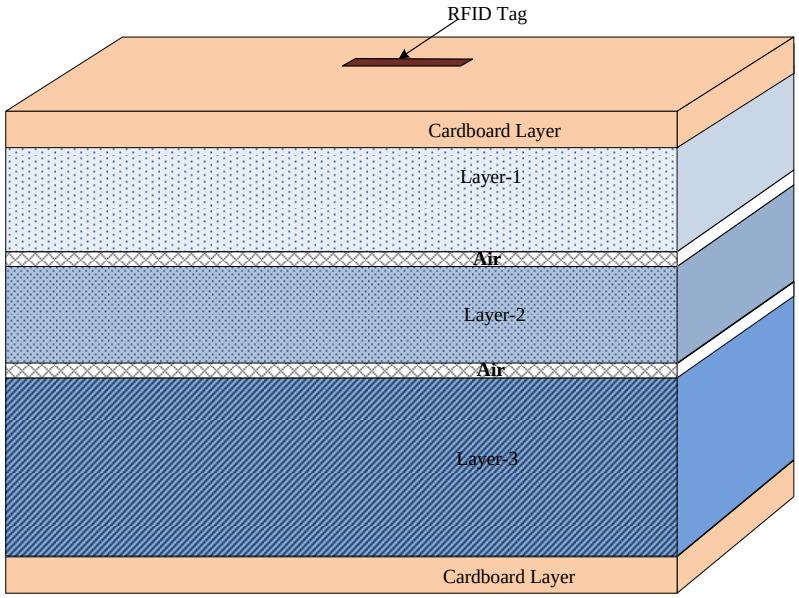

Figure 3.1. RFID tag on a cardboard box with various contents

The complex heterogenous environment of the box can be transformed to a homogenous medium of an equivalent dielectric constant. Now, to further simplyfy this model, the large box is assumed to be an *infinite slab* and let its relative permittivity be ϵ_r. Thus, in the *tag on slab* model, the dipole (tag antenna)is at the interface of the two half spaces i.e., air (*top*) and the *slab* (*bottom*). An ideal dipole is represented as two test charges (infinitesimal spheres one with positive charge $(+q)$ and the other with negative $(-q)$ charge) separated by a distance of d as shown in Figure. 3.2. There is electric field between these two charges. Let the capacitance between the two charges, in air be C_{air} and in the dielectric slab be C_{slab}.

The well known expression for capacitance between two infintesimally small spheres of equal radii,a, and separated by distance d, where $a \ll d$, in a medium

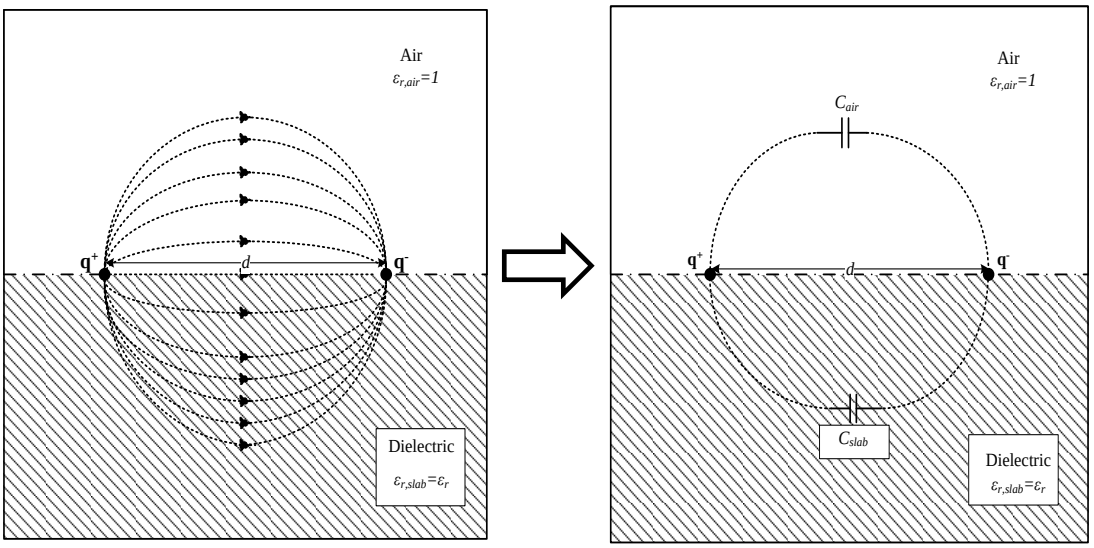

Figure 3.2. Half Space Model

of relative permittivity ϵ_r is

$$C = (4\pi\epsilon)\left(\frac{a^2}{d}\right)$$

where $\epsilon = \epsilon_0\epsilon_r$. The capacitance in each of the two half spaces, i.e., C_{air} and C_{slab} are given below

$$C_{air} = \frac{1}{2}\left[(4\pi\epsilon_0)\left(\frac{a^2}{d}\right)\right]$$
$$C_{slab} = \frac{1}{2}\left[(4\pi\epsilon_0\epsilon_r)\left(\frac{a^2}{d}\right)\right]$$

As seen in the Figure. 3.2, the capacitances C_{air} and C_{slab} are in parallel and

so the effective capacitance C_{eff} is given as

$$\begin{aligned} C_{eff} &= C_{air} + C_{slab} \\ &= 4\pi\epsilon_0 \left(\frac{a^2}{d}\right) \left[\left(\frac{1+\epsilon_r}{2}\right)\right] \end{aligned}$$

The expression for C_{eff} represents capacitance between two infintesimaly small spheres in dielectic medium of effective dielectric constant $\epsilon_{eff} = \frac{1+\epsilon_r}{2}$. The approximation for the effective permittivity of the homogenoues medium to represent half space case has been used in many texts [11–13]. We conclude that the half-space model can be represented as a homogenous medium with effective dielectric constant of ϵ_{eff} and this holds true for all charge distributions like planar strips, wire or spheres. This is an example for a heterogenous environment tranformation to an equivalent homogenous medium. Hence, for the rest of this thesis, we will consider the UHF RFID antenna immersed in a lossless homogenous medium to simplify further analysis and optimization.

According to the wave theory, the frequency f and wavelength λ of a EM wave are inversely proportional and are related as

$$v = f\lambda \tag{3.1}$$

where v is the speed of the wave in the medium and is given as

$$v = \frac{1}{\sqrt{\mu_0\mu_r\epsilon_0\epsilon_r}} \tag{3.2}$$

where permeability and permittivity of the free space is μ_0 and ϵ_0 respectively.

For the medium, the relative permeability is μ_r and the relative permittivity is ϵ_r. When the wave enters a new medium its speed changes and so does its wavelength as the frequency is constant.

Consider a wave with some frequency f travelling in free space ($\epsilon_r = 1$ and $\mu_r = 1$). Its wavelength denoted by λ and from (3.1) and (3.2), it is

$$\lambda = \frac{1}{f\sqrt{\mu_0\epsilon_0}} \tag{3.3}$$

Consider another wave travelling in medium of relative permittivity ϵ_r and let the frequency be f'. The wavelength of this wave is represented as λ' and it is given as

$$\lambda' = \frac{1}{f'\sqrt{\mu_0\epsilon_0\epsilon_r}} \tag{3.4}$$

For the two waves to have the same wavelength, i.e., $\lambda = \lambda'$, we get the relation between the freqency of the two waves as (3.5) by dividing (3.4) by (3.3) and rearranging

$$f' = f\sqrt{\epsilon_r} \tag{3.5}$$

As observed from the classic theory for analyzing T-match, the input impedance is addressed as a function of frequency. For example, the wave number β ($= \frac{2\pi}{\lambda}$) in Z_d is a frequency-dependent term. Hence, we use the relationship between the frequency and the permittivity of the medium given by (3.5) and obtain the transformation between the frequency and immersion in dielectric medium. As we know, the fields of a dipole antenna can be categorized as radiating and reactive (electric and magnetic) fields. We analyze the effect of immersion on frequency, by understanding and analyzing its effect on the fields that constitute the dipole.

3.2 Immersed Uda model

In the "immersed Uda model," for an antenna in a dielectric medium with relative permittivity ϵ_r, we can perform the following analysis. First, consider the radiating resistance R_r of an infinitesimal dipole with length l at some frequency f and immersed in a medium with relative permittivity ϵ_r. We start with the formulation from Balanis [7].

$$\begin{aligned} R_r(f;\ \epsilon = \epsilon_0\epsilon_r) &= \sqrt{\frac{\mu}{\epsilon_0\epsilon_r}}\left(\frac{2\pi l}{3}\right)\left(\frac{1}{\lambda}\right)^2 \\ &= \sqrt{\frac{\mu}{\epsilon_0\epsilon_r}}\left(\frac{2\pi l}{3}\right)(f\sqrt{\mu\epsilon_0\epsilon_r})^2 \\ &= \frac{R_r(f\sqrt{\epsilon_r};\ \epsilon = \epsilon_0)}{\sqrt{\epsilon_r}} \end{aligned}$$

Using the analysis given above, we observe that the radiating resistance of a dipole immersed in a dielectric with relative permittivity ϵ_r and at frequency f is that of the radiating resistance at frequency $f\sqrt{\epsilon_r}$ and scaled by a factor $\epsilon_r^{-1/2}$.

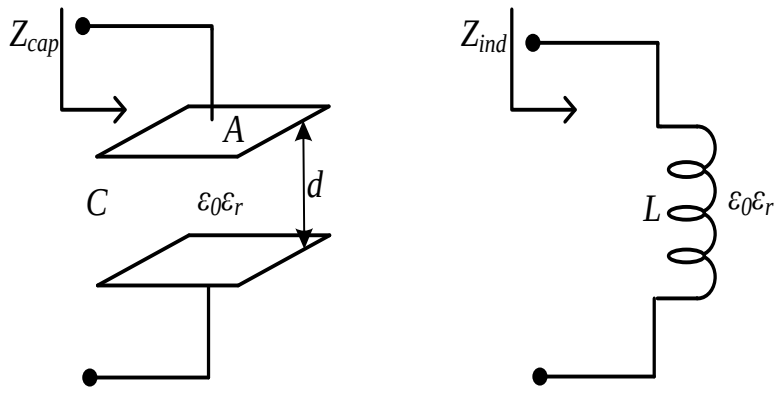

Figure 3.3. Capacitor and Inductor immersed in dielectric medium

Similarly, consider reactive fields of the antenna in terms of capacitance (elec-

tric) and inductance (magnetic) fields, separately. Let the impedance across a thin parallel plate capacitor with plate area A and plate separation d, immersed in a dielectric with relative permittivity ϵ_r be Z_{cap}, given by $(j\omega C)^{-1}$. Substituting the well known expression $C = \frac{\epsilon_0 \epsilon_r A}{d}$ in Z_{cap}, writing in f instead of ω and rearranging, we get

$$\begin{aligned} Z_{cap}(f;\ \epsilon = \epsilon_0\epsilon_r) &= \frac{d}{j2\pi f \epsilon_0 \epsilon_r} \\ &= \frac{d}{j2\pi (f\sqrt{\epsilon_r})\epsilon_0} \left(\frac{1}{\sqrt{\epsilon_r}}\right) \\ &= \frac{Z_{cap}(f\sqrt{\epsilon_r};\ \epsilon = \epsilon_0)}{\sqrt{\epsilon_r}} \end{aligned}$$

We observe that this identity follows the same form as the radiating resistance.

Next, we consider an inductor with inductance L immersed in dielectric medium. The reactance of the inductor is given by $Z_{ind} = j\omega L$, and has no dependance on the permittivity of the medium. However, we can still show the same identity.

$$\begin{aligned} Z_{ind}(f;\ \epsilon = \epsilon_0\epsilon_r) &= j2\pi f L \\ &= \frac{j2\pi (f\sqrt{\epsilon_r})L}{\sqrt{\epsilon_r}} \\ &= \frac{Z_{ind}(f\sqrt{\epsilon_r};\ \epsilon = \epsilon_0)}{\sqrt{\epsilon_r}} \end{aligned}$$

Thus, we find that radiating resistance, inductive, and capacitive components of the antenna immersed in a dielectric medium follow the same scaling. Thus, if we assume a perfect conductor and lossless dielectric medium, we can perform the impedance scaling to input impedance Z_{in} of any circuit consisting of radiating

resistance, capacitance and inductance.

$$Z_{in}(f;\ \epsilon_0\epsilon_r) = \frac{Z_{in}(f\sqrt{\epsilon_r};\ \epsilon_0)}{\sqrt{\epsilon_r}}$$

Note that this is an identity that states that input impedance of any circuit, at frequency f and immersed in a dielectric with relative permittivity ϵ_r is same as impedance of the same circuit operating at frequency $f\sqrt{\epsilon_r}$ and scaled by a factor $\epsilon_r^{-1/2}$.

The common mode impedance of a dipole, which is sum of the radiating and reactive fields, follows the same identity. We expect the input impedance of a short circuited lossless transmission line (represented as distributed series inductances and capacitances) to follow the same identity as well. As the equipotential line of a transmission line is unperturbed by the permittivity, we claim without proof, that the splitting factor of a transmission line, α also remains unaffected. We may thus conclude the following.

$$\begin{aligned} Z_c(f;\ \epsilon_0\epsilon_r) &= \frac{Z_c(f\sqrt{\epsilon_r};\ \epsilon_0)}{\sqrt{\epsilon_r}} \\ Z_d(f;\ \epsilon_0\epsilon_r) &= \frac{Z_d(f\sqrt{\epsilon_r};\ \epsilon_0)}{\sqrt{\epsilon_r}} \\ Z_{in}(f;\ \epsilon_0\epsilon_r) &= \frac{Z_{in}(f\sqrt{\epsilon_r};\ \epsilon_0)}{\sqrt{\epsilon_r}} \end{aligned} \tag{3.6}$$

Note again that α is not a function of frequency or relative permittivity.

The (3.6) gives the relation of frequency to immersion in dielectric transformation. (3.6) for common, differential, and input impedance of the antenna constitutes the Immersed Uda Model. Before we use this relation to analyze a UHF

RFID tag antenna in dielectric, we validate the relation by the following simple experiment.

3.2.1 Validation

The Immersed Uda Model presented in Section 3.2 will be used to make several predictions, which we use in analysis for optimization. So, we first aim to validate frequency dielectric transformation in (3.6). For this, we selected a typical T-match dipole antenna and simulated two scenarios: one in which we kept the antenna in air and swept frequency over a broad range, and the second in which we kept the frequency fixed but immersed the antenna in a changing permittivity medium. Essentially, we are changing the wavelength in the two cases. The purpose was to directly test (3.6).

Recall the antenna shown in Figure. 5.2. The dimensions of the antenna are set to $L = 100$ mm, $W = 8$ mm, $W_1 = W_2 = 3.5$ mm, $M = 1$ mm. For the first case we simulated the antenna in air and swept it over frequencies from 915 MHz to 2 GHz. Next, we place the same antenna in a dielectric box of dimensions $(400 \times 400 \times \times 400)$ mm and vary the dielectric constant from 1 to 5 in steps of 0.5. We report both R_{in} and X_{in} for two cases:

- Immersion, i.e., $Z_{in}(f, \epsilon_r\epsilon_0)$.
- Full scaling according to (3.6), i.e., $Z_{in}(f\sqrt{\epsilon_r};\ \epsilon_0)/\sqrt{\epsilon_r}$.

The results are presented in Figure. 3.4. Clearly, we see that the immersion and impedance scaling show excellent agreement. We can conclude that (3.6) is an excellent approximation, and that differences may be due more attributed to simulation accuracy than anything else. Hence, the Immersed Uda Model very

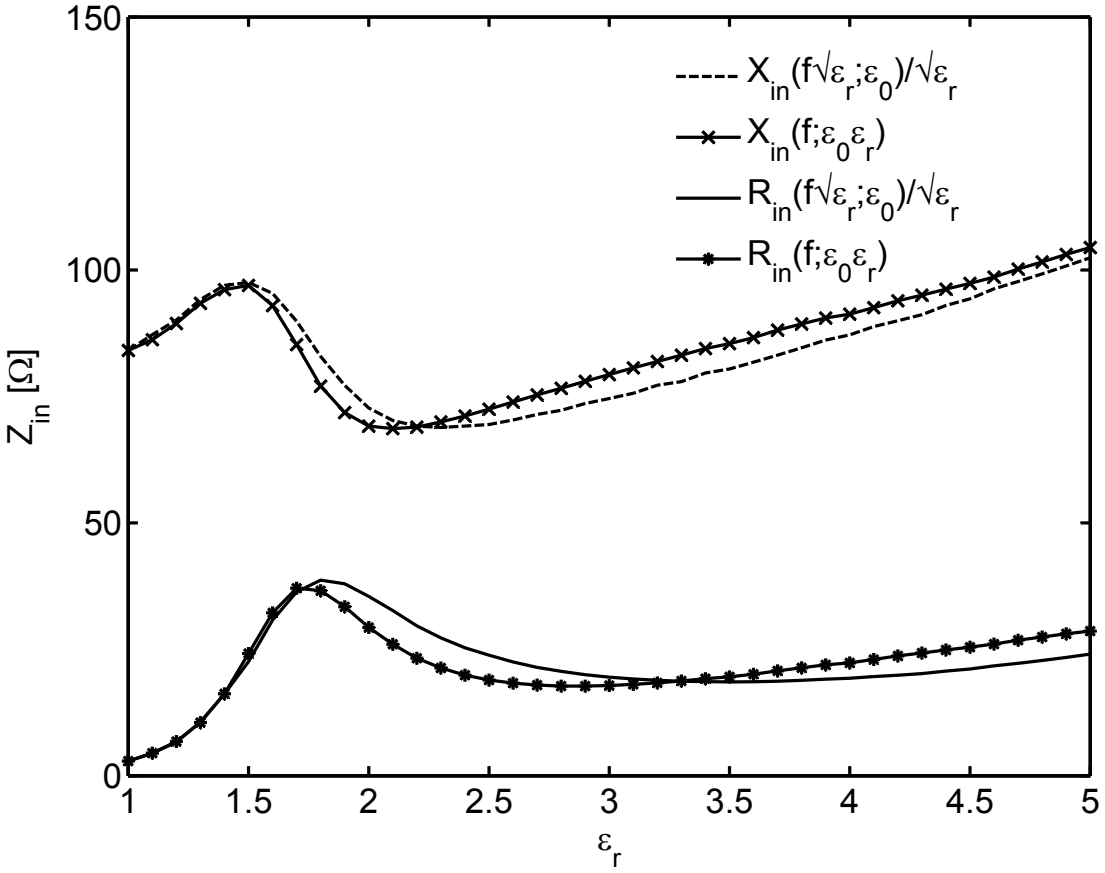

Figure 3.4. Experimental results validating (3.6).

accurately predicts the input impedance of a T-match antenna immersed in a lossless homogeneous dielectric medium.

In this chapter, we developed a model that is useful for optimizing the antenna design for homogeneous environments. Now that we have a formal model, we analytically solve for solution for the ideal case and numerically analyze the practical case in detail in the next chapter.

Chapter 4

Analysis

So far, we have derived and validated the frequency dielectric transformation in *Immersed Uda Model*. This model is analyzed to obtain optimality condition for the antenna in dielectric environments in Section. 4.1. To improve accuracy of the model, an equivalent circuit useful for computation of the input impedance of center-fed ribbon dipole is presented Section. 4.2. In Section. 4.3, we introduce a the term "dielectric-bandwidth" and propose a numerical method, based on brute-force search, to obtain a robust tag antenna for a given power transfer effciency coefficient τ_{min}.

4.1 Analytical Approach

For further analysis of the antenna using the immersed Uda model, we need a tractable closed form expression for common mode impedance Z_c. Typically, RFID antennas operate in region below and near first resonance. It is well-known that the impedance of a dipole below and near first resonance can be approximated as a series RLC circuit. Thus, for simplicity, let us assume Z_c behaves like a series

RLC circuit consisting resistor R_c, inductor L_c, and capacitor C_c. Then we have

$$Z_c = R_c + j2\pi f L_c + \frac{1}{j2\pi f C_c} \tag{4.1}$$

The Uda model with the RLC circuit for Z_c is given in Figure. 4.1.

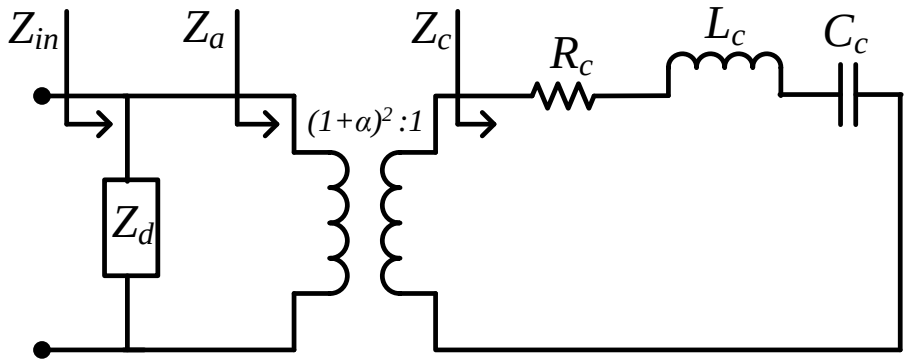

Figure 4.1. Uda equivalent circuit using series RLC circuit for dipole common mode.

Now that we have a formal model, consider the antenna immersed in a dielectric medium. One criteria to analyze a antenna that could be both useful and tractable to analyze is one that is both perfectly matched and unperturbed by being immersed in dielectric medium with small permittivity. For a given IC, τ can be made a function of both frequency and dielectric. We can formalize these conditions as follows.

1. $\tau(f = 915\,\text{MHz};\ \epsilon = \epsilon_0) = 1.$

2. $\frac{\partial \tau}{\partial \epsilon_r}\ |_{\epsilon_r=1} = 0.$

Simply, these conditions state that the power transfer efficiency is perfect in a vacuum at the frequency of interest (e.g., 915 MHz), and that small changes

in the relative permittivity of the immersed medium (e.g., immersion in a light foam) will not change τ. For the remainder of this chapter, we will examine the consequences of these two conditions. Specifically, we will deduce the relationship between the Q of the antenna (in the common mode) and Z_0, the characteristic impedance of the differential mode.

To satisfy the first condition $\tau(f = 915\,\text{MHz};\ \epsilon = \epsilon_0) = 1$, the input impedance of the antenna Z_{in} should be complex conjugate of the chip impedance Z_{ic}. Given a common mode impedance Z_c and a chip impedance Z_{ic}, the required α and Z_d to create $Z_{in} = Z_{ic}^*$, can be expressed as follows [4].

$$Z_d = -j\frac{R_c(R_{ic}^2 + X_{ic}^2)}{R_c X_{ic} + R_{ic} X_c}$$
$$\alpha = \sqrt{\frac{R_c(R_{ic}^2 + X_{ic}^2)}{R_{ic}(R_c^2 + X_c^2)}} - 1$$

Recall that the differential mode is twice the impedance of a shorted transmission line with length $S/2$. Given a required Z_d, it is straightforward to find a suitable slot length S.

$$S = \frac{2}{\beta}\tan^{-1}\left(\frac{X_d}{2Z_0}\right) \tag{4.2}$$

Obviously, we are interested in the smallest positive S.

Given the common mode impedance Z_c, the parameters Z_d and α are prescribed. Said another way, the Uda model prescribes a certain α and Z_d; there are no choices. However, there are two important variables within the Uda model: the resonant frequency of the dipole antenna f_0, and the characteristic impedance of the transmission line Z_0. In our embedded-T antenna from Figure. 5.2, f_0 can be manipulated by changing the length of the antenna and Q by the total width. In practice, the dipole arms can include meandering lines that can be used

to increase the electrical length in a confined space. Z_0 can be manipulated by changing M (see Figure. 5.2); a wider gap will result in a larger Z_0.

Let us assume that our antenna form factor is limited in such a way so as to prescribe an antenna Q and R_c. We are thus constrained by a prescribed α and Z_d. We are left with only two degrees of freedom: f_0 and S.

Note that if $\frac{\partial \tau}{\partial \epsilon_r} \mid_{\epsilon_r=1} = 0$, then $\frac{\partial Z_{in}}{\partial \epsilon_r} \mid_{\epsilon_r=1} = 0$. Obviously, Z_{in} can be expressed as a sum of resistance and reactance i.e., $Z_{in} = R_{in} + jX_{in}$. Substituting (2.4) and $Z_d = jX_d$ in (2.3), we get Z_{in} as

$$Z_{in} = \frac{Z_a Z_d}{Z_a + Z_d} = \frac{R_a X_d^2}{R_a^2 + (X_a + X_d)^2} + j\frac{R_a^2 X_d + X_a X_d (X_a + X_d)}{R_a^2 + (X_a + X_d)^2} \tag{4.3}$$

We know that input resistance R_{in} has only one zero in its slope, and that it occurs near f_0, so for now let us assume common mode is resonant at the operating frequency f, and thus $X_c \approx X_a \approx 0$ for at $f = 915$ MHz and $\epsilon_r = 1$. Also, $\frac{\partial R_{in}}{\partial \epsilon_r} \mid_{\epsilon_r=1} = 0$ at $f_0 = f = 915$ MHz.

So, we now solve for $\frac{\partial X_{in}}{\partial \epsilon_r} \mid_{\epsilon_r=1} = 0$. for the second condition. From (4.3), the input reactance can be expressed as follows.

$$X_{in} = \frac{R_a^2 X_d + X_a X_d (X_a + X_d)}{R_a^2 + (X_a + X_d)^2}$$

Differentiating X_{in} with respect to ϵ_r and substituting $X_a = 0$, we get the follow-

ing.

$$\begin{aligned}\frac{\partial X_{in}}{\partial \epsilon_r} &= R_a^2 \left(\frac{\partial X_d}{\partial \epsilon_r}\right) + X_d^2 \left(\frac{\partial X_a}{\partial \epsilon_r}\right) \\ &\quad - \frac{2R_a^2 X_d^2}{R_a^2 + X_d^2} \left(\frac{\partial X_a}{\partial \epsilon_r} + \frac{\partial X_d}{\partial \epsilon_r}\right) \\ &= \left(R_a^2 \left(\frac{\partial X_d}{\partial \epsilon_r}\right) - X_d^2 \left(\frac{\partial X_a}{\partial \epsilon_r}\right)\right) \left(\frac{R_a^2 - X_d^2}{R_a^2 + X_d^2}\right)\end{aligned} \tag{4.4}$$

Setting the partial derivative of X_{in} at $\epsilon_r = 1$ to zero, i.e., $\frac{\partial X_{in}}{\partial \epsilon_r} \mid_{\epsilon_r=1} = 0$. we get,

$$R_a^2 \left(\frac{\partial X_d}{\partial \epsilon_r}\right) \mid_{\epsilon_r=1} = X_d^2 \left(\frac{\partial X_a}{\partial \epsilon_r}\right) \mid_{\epsilon_r=1} \tag{4.5}$$

as $\frac{R_a^2 - X_d^2}{R_a^2 + X_d^2} \neq 0$. Note that this expression (4.5) includes terms $\frac{\partial X_a}{\partial \epsilon_r}$ and $\frac{\partial X_d}{\partial \epsilon_r}$, which we investigate next.

Since we express the common mode impedance as a series RLC circuit, we can express Z_c in terms of R_c, Q, and $\omega_0 = 2\pi f_0$. In particular, the expression for the reactance is [23]

$$X_c = R_c Q \left(\frac{\omega}{\omega_0} - \frac{\omega_0}{\omega}\right) .$$

When immersed in a dielectric medium, the common mode reactance is scaled as follows.

$$X_c(\omega;\ \epsilon_r) = R_c Q \left(\frac{\omega\sqrt{\epsilon_r}}{\omega_0} - \frac{\omega_0}{\omega\sqrt{\epsilon_r}}\right) \frac{1}{\sqrt{\epsilon_r}}$$

Differentiating with respect to ϵ_r and simplifying, we get the following.

$$\frac{\partial X_c}{\partial \epsilon_r} \mid_{\epsilon_r=1} = R_c Q$$

Similarly,

$$\frac{\partial X_a}{\partial \epsilon_r} \mid_{\epsilon_r=1} = (1+\alpha)^2 R_c Q \, . \tag{4.6}$$

Next, let us consider the affect of ϵ_r on Z_d. Recall

$$Z_d = jX_d = j2Z_0 \tan\left(\frac{\beta S}{2}\right) . \tag{4.7}$$

Differentiating, we get the following.

$$\begin{aligned}\frac{\partial X_d}{\partial \epsilon_r} &= \frac{\partial}{\partial \epsilon_r}\left(\frac{1}{\epsilon_r} 2Z_0 \tan\left(\frac{\beta_0\sqrt{\epsilon_r}S}{2}\right)\right) \\ &= -\frac{2Z_0}{\epsilon_r^2}\tan\left(\frac{\beta_0\sqrt{\epsilon_r}S}{2}\right) \\ &\quad - 2Z_0 \sec^2\left(\frac{\beta_0\sqrt{\epsilon_r}S}{2}\right)\frac{\beta_0 S}{2\sqrt{\epsilon_r}}\end{aligned}$$

Evaluating the partial derivative of X_d at $\epsilon_r = 1$, we get,

$$\frac{\partial X_d}{\partial \epsilon_r} \mid_{\epsilon_r=1} = -2Z_0 \tan\left(\frac{\beta_0 S}{2}\right) + \frac{Z_0\beta_0 S}{2}\sec^2\left(\frac{\beta_0 S}{2}\right)$$

We substitute (4.2) for S and (4.7) in the above expression. Using the *identity* $sec^2(x) = 1 + tan^2(x)$ and rewriting the expression only in terms of X_d and Z_0 as

$$\frac{\partial X_d}{\partial \epsilon_r} \mid_{\epsilon_r=1} = -X_d + Z_0\left(1 + \left(\frac{X_d}{2Z_0}\right)^2\right)\tan^{-1}\left(\frac{X_d}{2Z_0}\right) \tag{4.8}$$

We now have the two terms $\frac{\partial X_a}{\partial \epsilon_r}$ and $\frac{\partial X_d}{\partial \epsilon_r}$ evaluated at $\epsilon_r = 1$ i.e., (4.6) and (4.8) respectively. Recall the expression in (4.5) obtained by setting the partial derivative $\frac{\partial X_{in}}{\partial \epsilon_r}$ to zero (the second condition). Substituting (4.6) and (4.8) in (4.5) and re-arranging the terms, we arrive at the final expression in (4.9).

$$Z_0\left(1 + \left(\frac{X_d}{2Z_0}\right)^2\right)\left(\tan^{-1}\left(\frac{X_d}{2Z_0}\right)\right) = \frac{X_d^2 Q}{(1+\alpha)^2 R_c} + X_d \tag{4.9}$$

From the final expression, it is difficult to find a closed form solution, so we solve the above numerically for several typical cases. Let $Z_{ic} = 18 - j165\,\Omega$. Furthermore, we relax the constraint that the common mode is resonant to find exact solutions. We found that for $Q = 5$, $Z_0 = 37\,\Omega$; for $Q = 15$, we find that $Z_0 = 22\,\Omega$; and for $Q = 25$ we find that $Z_0 = 16\,\Omega$. From this, we can deduce that Q and Z_0 are inversely proportional. More importantly, we notice that Z_0 in the range of a few tens of Ohms is *impractical* to implement with coplanar strips. The smallest realizable Z_0 is approximately $80\,\Omega$ with a gap a few hundred microns wide. For a typical 100 mm dipole tag with $Q \approx 15$, a Z_0 of 22 Ω is simply impossible to construct. Thus, we must conclude that while a theoretical solution exists for this condition, it is simply not practical to construct an antenna with those two criteria.

One way to interpret this result is that the reactance of the common mode has a relatively large slope, and the slope of the differential mode impedance must be made sufficiently large to compensate. This large slope is only achievable when the shorted transmission line is near $\lambda/4$. To achieve a large slope for a given, relatively small Z_d, one must use a small Z_0. Unfortunately, one can only decrease Z_0 so small before it is not possible to physically realize such a small Z_0 using simple printed manufacturing techniques. Thus, we next explore an approach based on an exhaustive search over the parameter space, constrained by physical parameters that are possible to be physically realized in Section. 4.3.

One major assumption in this analysis is that the common mode impedance is the input impedance of a series RLC network. As stated earlier, this model is applicable in regions below and near resonance only. This restricts the bandwidth that is needed to accurately determine the "optimal" antenna using numerical

approach. Therefore, in the next Section. 4.2, we introduce a five element circuit equivalent circuit model for common mode impedance Z_c.

4.2 An Equivalent Circuit for Common Mode Impedance

In this section, we discuss a more sophisticated, multi-resonant circuit model for the computation of Z_c. We also propose a method to use this model to compute Z_c for varying antenna structures with a fixed form factor.

Hamid et. al. [24] derive an equivalent circuit to compute the input impedance (Z_c) of a center-fed wire dipole of arbitrary length. The equivalent circuit consists of a series LC network in series with cascaded parallel RLC networks as shown in Figure. 4.2. The number of parallel networks is determined by the ratio of length of the antenna and the wavelength or by the number of modes one intends to model.

In this thesis, we use a five element equivalent circuit to compute the input impedance Z_c of a center-fed ribbon dipole. The computation is done for the first two octaves, therefore, only one parallel RLC network is considered. The equivalent circuit is shown in Figure. 4.2 [24]. The impedance of series L_{c0} and C_{c0} is represented as Z_{c0} and impedance of parallel R_{c1}, L_{c1} and C_{c1} as Z_{c1}. The input impedance (Z_c) of the equivalent circuit is given as (4.10)

$$Z_c = Z_{c0} + Z_{c1} = j2\pi f L_{c0} + \frac{1}{j2\pi f C_{c0}} + \frac{1}{\frac{1}{R_{c1}} + \frac{1}{j2\pi f L_{c1}} + j2\pi f C_{c1}}. \qquad (4.10)$$

The first resonance of the dipole is represented as f_0, which is approximately equal to the resonance of the series LC network. The second resonance, f_1, of the dipole is determined by the resonance of parallel RLC network. The process

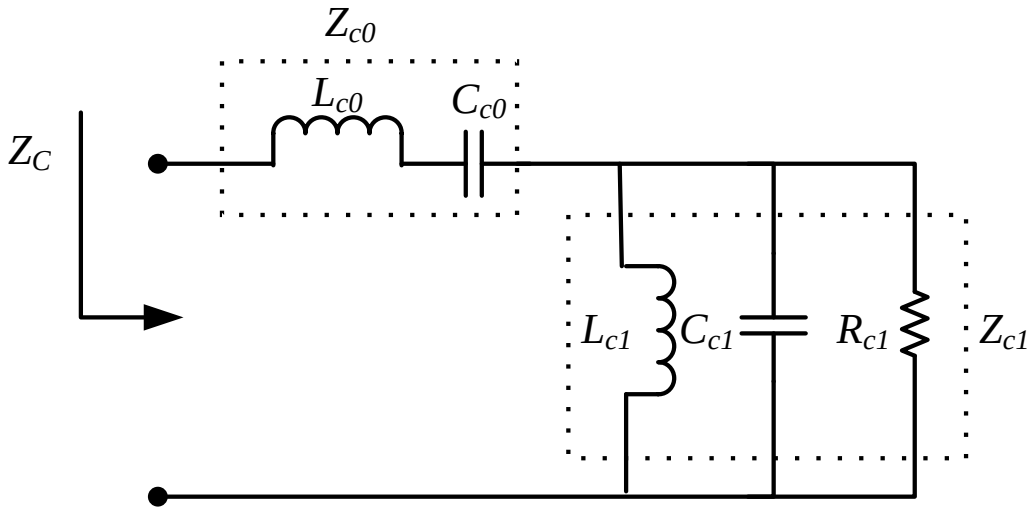

Figure 4.2. The Equivalent Circuit Model for Z_c

(explained later) to compute the circuit elements in Figure. 4.2 is dependent on either closed form solutions of Z_c or numerical solvers. As closed form solutions for fat ribbon dipoles and meandered antennas do not exist, we use HFSS to determine the dipole impdeance vs frequency, which in turn we use it to compute the circuit elements. The process to compute the equivalent circuit elements is as follows:

1. The given antenna is center-fed and simulated over the range of frequencies from 800 MHz to 1.8 GHz.

2. Determine the input impedance and the resonate frequencies (f_0 and f_1).

3. The peak of the input resistance is taken as R_{c1}.

4. Determine -3 dB bandwidth (BW) and compute Q factor ($Q = \frac{f_1}{BW}$).

5. C_{c1} and L_{c1} are then computed using the following equations:

$$f_1 = \frac{1}{2\pi\sqrt{C_{c1}L_{c1}}},$$
$$Q = \frac{1}{R_{c1}}\left(\sqrt{\frac{L_{c1}}{C_{c1}}}\right).$$

6. The first resonance f_0, the intercept point of the reactance X_c curve at the first resonance are used and then curve fitting technique is applied to compute C_{c0} and L_{c0} accurately.

It is well known that the resonant frequency of a dipole is inversely proportional to the length of the dipole. Since one of the major constraints of RFID tag antennas is the form factor of the antenna, in order to lower the resonant frequency of the dipole of a fixed form factor, meanders and tip loading [1] can be applied. Observe that, the resonant frequency achieved for a simple dipole (without meanders) is the maximum possible resonant frequency for the given form factor. An antenna with meanders is shown in Figure. 4.3. The resonant frequency of the antenna can be changed by varying the number of meanders added. The number of meanders are controlled by the trace width ΔW of the meanders. Hence, for a given form factor, by varying the number of meanders, a large set of antenna structures with varying resonant frequencies is possible. We propose to compute the equivalent circuit elements of three antennas, in the large set, and use curve fitting technique (quadratic) to determine the equivalent circuit elements of all the other antenna structures in that set. The three antennas are selected such that their first resonant frequencies are $f_{0,min}$, $f_{0,mid}$ and $f_{0,max}$, where $f_{0,min}$ is the minimum resonant frequency achievable for the given form factor, $f_{0,max}$ is the maximum and $f_{0,mid}$ is the mid-point of the two.

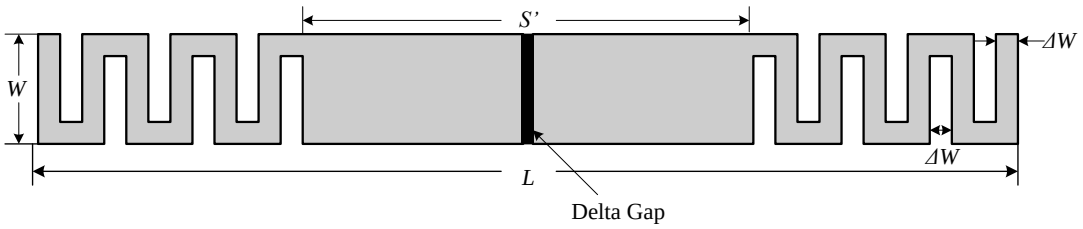

Figure 4.3. Antenna with Meander lines

We implement this process for a tag antenna of given form factor $L = 100$ mm and $W = 8$ mm. For an Embedded T-match antenna, as a slot is embedded in the antenna, we add meanders to the antenna beyond S'as shown in Figure. 4.3. S' is considered to be approximately $\lambda/8$. Recall that the trace width ΔW is used to vary the number of meanders. The minimum physically realizable ΔW of 0.5 mm gives the antenna structure with $f_{0,min}$ resonant frequency. The antenna structure with no meanders has a resonant frequency $f_{0,max}$ and experimentally it was found that the antenna structure with ΔW of 1 mm yields resonant frequency of $f_{0,mid}$.

The process to compute the equivalent circuit elements is then implemented for the three antennas. The antennas are simulated over a frequency range of 800 MHz to 1.8 GHz in step size of 5 MHz in HFSS. The equivalent circuit elements of the three antennas is tabulated in Table 4.1.

First Resonant Frequency [MHz]	L_{c0} [nH]	C_{c0} [pF]	R_{c1} [Ω]	L_{c1} [nH]	C_{c1} [pF]
$f_{0,min} = 912.4$	4.42	77.87	893.09	11.64	1.78
$f_{0,min} = 1176$	1.28	81.67	449.69	9.35	1.22
$f_{0,min} = 1413$	2.82e−4	89.87	273.05	8.60	0.85

Table 4.1. Equivalent Circuit Model Elements.

The *polyfit* function in *MATLAB* is used to generate quadratic expression in

first resonant frequency f_0 for each of the five circuit elements using the computed values of the elements in Table. 4.1. The quadratic expressions take the first resonant frequency f_0 of a given antenna structure as input and give the corresponding equivalent circuit elements. Using the five quadriatic expressions, the equivalent circuit for each of the antenna structures in the large set for a given form factor (100 mm $\times$ 8 mm) can be determined. This procedure is validated in following section.

4.2.1 Validation

Recall, the antenna design shown in Figure. 4.3. Consider one such antenna with meanders with trace width 0.75 mm. We simulated this antenna in air and swept over the frequency range 800 MHz to 1.8 GHz. We obtain the first resonance from the simulation result. Now, using *polyeval* function in MATLAB at the given f_0, the five elements namely L_{c0}, C_{c0}, R_{c1}, L_{c1} and C_{c1} of the equivalent circuit are determined from their corresponding quadriatic equations in Section 4.3. The equivalent circuit, thus obtained, is used to predict the input impedance of the antenna for the same frequency range of 800 MHz to 1.8 GHz.

We compare the input resistance and reactance of the antenna predicted by the electrical model with the simulation result in the plots in Figure. 4.4 and Figure. 4.5. We observe that the input impedance i.e., resistance and reactance line up well for the lower frequency range 800 MHz to 1.4 GHz. For the frequency range of 1.4 GHz to 1.8 GHz, the error seems to increase but it is well below 10%. The minor error can be attributed to the inaccuracy while curve fitting. And, thus there is scope of improvement. Note that the model is accurate for the UHF operating range of 860–960 MHz.

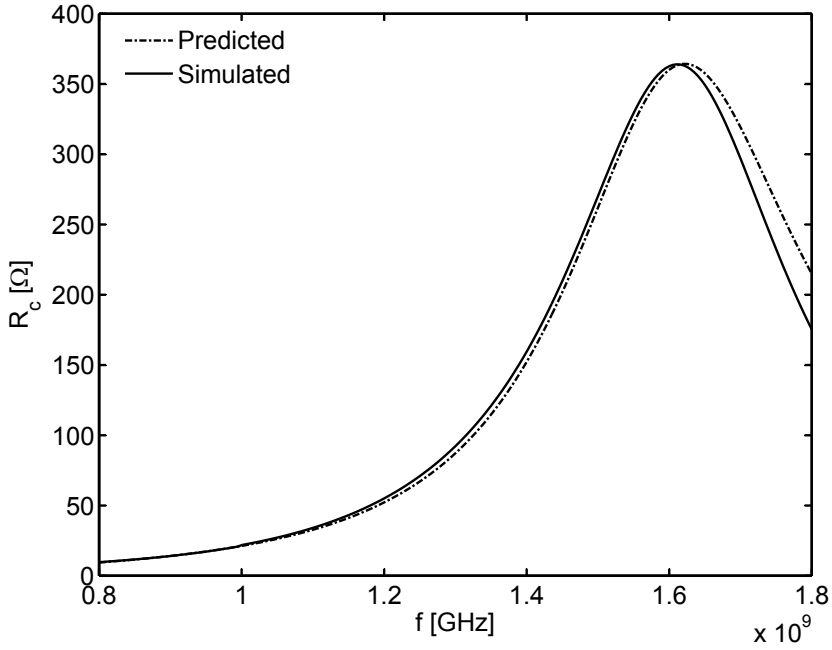

Figure 4.4. Experimental Results comparing the Input Resistance R_c predicted by electrical model and simulation results.

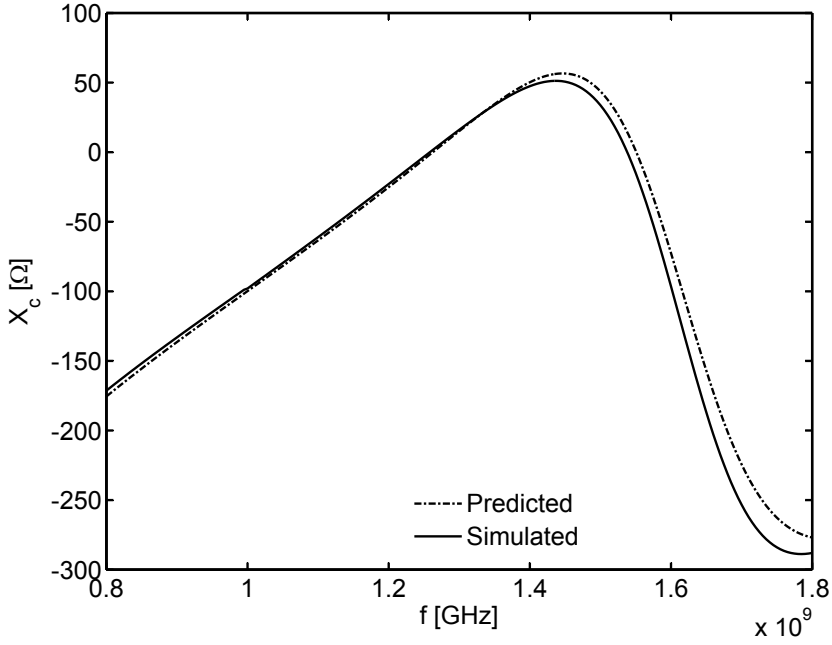

Figure 4.5. Experimental Results comparing the Input Reactance X_c predicted by electrical model and simulation results.

Hence, we conclude that the five element circuit model for the common mode impedance of the strip dipole serves the purpose well and so will be used in the parametric search done in the next section.

4.3 Numerical Approach

In this section, we approach the new model with a realistic set of bounds on the parameters like resonant frequency f_0, α, characteristic impedance in differential mode Z_0 and slot length of the antenna S and run a exhaustive parametric search for the best possible fit.

For this, let us define a more practical constraint than the one used in the section 4.1. We say that an antenna, operating at a frequency f, has a *dielectric-bandwidth* of $(\epsilon_{r,u} - \epsilon_{r,l})$ if $\tau(f;\ \epsilon_r) \geq \tau_{min}$, $\forall \epsilon_r \in [\epsilon_{r,l}, \epsilon_{r,u}]$. That is, the dielectric bandwidth is the range of permittivity values for which the antenna can be immersed in and provide a given level of power transfer efficiency τ_{min}. Here, $\epsilon_{r,l}$=1, therefore, *dielectric-bandwidth* is $\epsilon_{r,u} - 1$.

In this experiment, we assume Z_{ic} to be $18 - j165$ at the operating frequency of $f = 915$ MHz. The bounds on first resonance frequency f_0, for a fixed form factor, are determined as outlined in the previous section. The program in MATLAB to obtain the best fit is presented in the form of pseudocode. In this code given below, we use the term f_{ratio} instead of the resonant frequency as required by MATLAB, for the calculation of the equivalent circuit elements. It is the ratio of the resonant frequency f_0 and the minimum possible resonant frequency $f_{0,min}$. The value of f_0 lies within the range $[f_{0,min},\ f_{0,max}]$. Recall that the form factor synthesized is 100 mm x 8 mm and the resonant frequency $f_{0,min}$ is 912.4 MHz and $f_{0,max}$ is 1.413 GHz. The five parameters namely C_{c0}, L_{c0}, C_{c1}, L_{c1} and R_{c1}

of the circuit model are evaluated from their corresponding quadriatic equations as outlined in previous section. We assume intial value of $\epsilon_{r,u}$ to be 1 and after every iteration it is updated to a new maximum value.

The constraints on slot length S is varied between values of 20 mm and 40 mm as the upper limit is prescribed by S' for the antenna structures represented by Figure. 4.3. Recall the embedded T-match antenna shown in Figure. 5.2. The width W and W_1, and gap M are varied within the physically realizable limits to obtain the bounds for Z_0 numerically using (2.6). Similarly, the limits on α are determined numerically using (2.9).

The input optimality condition to the program is the prescribed power transfer efficiency τ_{min} and the corresponding maximum possible value of $\epsilon_{r,u}$ is the output result. We present the results obtained for each of three values of $\tau_{min} = -1, -2,$ and -3 dB in Table. 4.2.

τ_{min} $[dB]$	$\epsilon_{r,u}$	f_0 [MHz]	Z_0 [Ω]	S [mm]	α
-1	1.24	972	205	39	3.5
-2	2.27	1087.2	200	37	2.1
-3	6.56	1413	220	31	1.5

Table 4.2. Results to compute dielectric-bandwidth for a given minimum power transfer efficiency τ_{min}.

From the Table. 4.2, we observe that the value of $\epsilon_{r,u}$ has an abrupt shift from 2.27 for $\tau_{min} = -2$ dB to 6.56 for $\tau_{min} = -3$ dB. To explore this phenomenon, we vary the input τ_{min} from 0.9 to 0.5 in steps of 0.05 and plot the corresponding $\epsilon_{r,u}$ with respect to τ_{min}. The following Figure. [4.6] shows $\epsilon_{r,u}$ vs τ_{min} plot.

From this plot Figure. 4.6, we infer that the maximum possible relative permitivity ($\epsilon_{r,u}$) is increasing non-linearly with respect to minimum power transfer efficiency. As we lower the required minimum power transfer efficiency, we can

Algorithm 1 Pseudocode for the MATLAB Program

```
for each f_ratio from 1 to 1.5486 at steps of 0.001 do
    Evaluate the Quadriatic Expressions for C_c0, L_c0, R_c1, C_c1, L_c1 at f_ratio
    From the equivalent circuit in Figure. 4.2, calculate Z_c at f using (4.10)
    for each S from 20 mm to 40 mm in steps of 1mm do
        for each Z_0 from 150Ω to 220Ω in steps of 5Ω do
            Calculate X_d at f using (2.5)
            for each α from 0.3 to 3 in steps of 0.1 do
                Calculate Z_in at f using (2.3)
                Calculate τ at f using (2.1)
                if τ ≥ τ_min then
                    for each ε_r from 1.01 to 10 in steps of 0.01 do
                        Calculate f_new using (3.5)
                        Calculate Z_c,new, X_d,new, and Z_in,new using (3.6) at f_new
                        Calculate τ_new
                        if τ_new ≥ τ_min and ε_r ≥ ε_r,u then
                            Assign the value of ε_r to the variable ε_r,u
                            Save the corresponding values of α, S, f_0, Z_0
                        else if τ_new <τ_min then
                            Break
                        end if
                    end for
                end if
            end for
        end for
    end for
end for
```

achieve antennas with better dielectric bandwidth i.e., $\epsilon_{r,u} - \epsilon_{r,l}$.

Hence, from the analysis conducted on the immersed Uda model, we observed that the most simple condition for optimality for an antenna immersed in dielectric is practically impossibe to satify. We approach the model with a physically realizable set of conditions and find the maximum possible relative permitivity for a given minimum power transfer efficieny. In the next chapter, we validate the electrical model proposed in Section. 4.3.

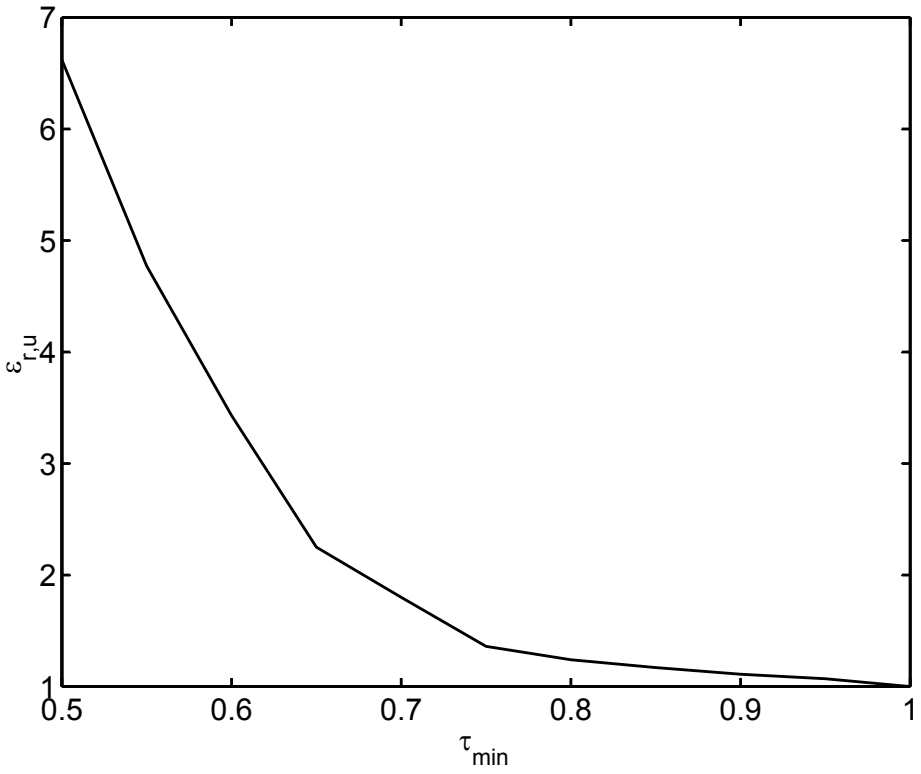

Figure 4.6. Maximum possible relative permitivity ($\epsilon_{r,u}$) vs Minimum Power transfer efficiency (τ_{min})

Chapter 5

Validation Result

The RFID tag antennas are generally designed in commercially available simulation tool. Ansys product suite - HFSS and Ansoft Designer, WIPL-D Microwave, CST Microwave Studio and Agilent Technologies - Advanced Design System (ADS) are few of the most commonly used simulation tools. In this thesis, the simulations for experiments and validation are done in HFSS *High Frequency Structure Simulator*, a industry-standard simulation tool for 3D full-wave electromagnetic field simulation. HFSS offers multiple state-of the-art solver technologies each based on the proven finite element method.

In this chapter, we present the final validation result of the model used in Section 4.3. To this end, we propose the following experiment. First, we construct (in HFSS) the antenna shown in Figure. 5.2. Next, we find the circuit-equivalent of the antenna. If the model is accurate, we would expect that the model-predicted input impedance will approximately match that of the antenna immersed in a dielectric medium. Also, for comparing the antenna to a commercially available tag, we use a baseline tag. For this, we use *Alien Squiggle*, shown in Figure. 5.1, a popular commercial tag as it is comparable to the optimal antenna design in

terms of form factor and Q-factor. We model the *Squiggle* in HFSS and subject it to the same simulation environment.

Figure 5.1. Alien Squiggle.

For this experiment, the following parameters were prescribed by the electrical model for $\tau_{min} = 0.5012$ $Z_0 = 215\,\Omega$, $S = 31$ mm $f_0 = 1.413$ GHz, and $\alpha = 1.5$, $R_1 = 273.0477\,\Omega$, $L_0 = 28.202\,pH$, $C_0 = 89.865\,pF$, $L_1 = 85.959\,nH$, $C_1 = 84.721\,pF$. The predicted $\epsilon_{r,u}$ is 6.4. We know that the form factor of the antenna is fixed to $L = 100$ mm and $W = 8$ mm. From the required Z_0 and α values, we use (2.6) and (2.9) to obtain $W_1 = 2.3$ mm, $W_2 = 4.2$ mm, $M = 1.5$ mm. In HFSS, the antenna is constructed using these dimensions, as shown in Figure. 5.2, and minor adjustments are made i.e., $S = 32$ mm (note the difference) to get the right slope of the differential mode impedance. This adjustment is required as the antenna is constructed with a 2 mm gap for the source which otherwise is ideally a delta gap.

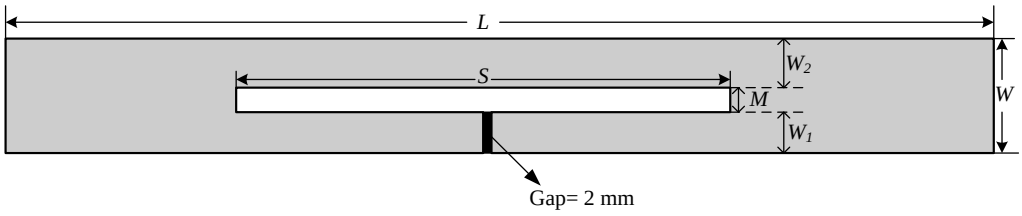

Figure 5.2. Optimal antenna design used in final validation.

Now, this antenna is simulated in a dielectric box of dimensions (400x400x400)

mm with relative permittivity of the medium varied from 1 (vaccum) to 6.4. The model is shown in Figure. 5.3. The length, breadth and the height of the box is greater than $\lambda = 324$ mm to avoid reflections at the radiation boundary and thereby create a pseudo-infinite environment filled with lossless homogeneous dielectric material. The baseline tag is also simulated in the same simulation environment. The predicted and simulated values of power transfer efficiency τ_{min}

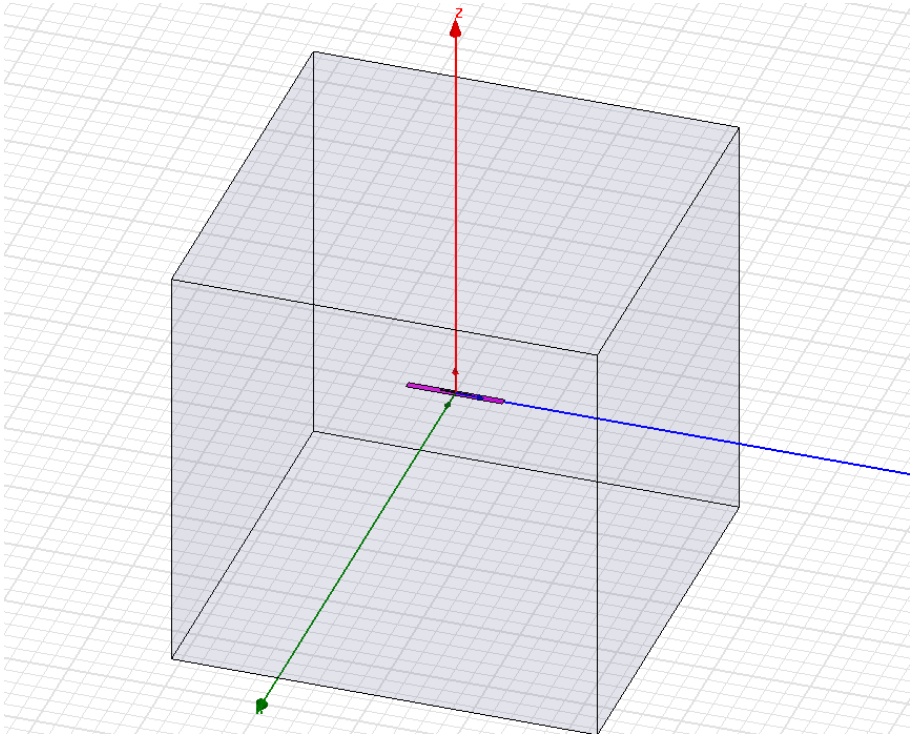

Figure 5.3. Experimental setup in HFSS.

of the optimal antenna design over the dielectric range of 1 to 6.4, are compared with each other. The simulated results of the optimal antenna is also compared with that of the baseline tag in Fig. 5.4. We see a good agreement between the predicted and simulated results. The minor dip in the simulated result curve of the optimal curve can be attributed to the error due to the source gap. For small

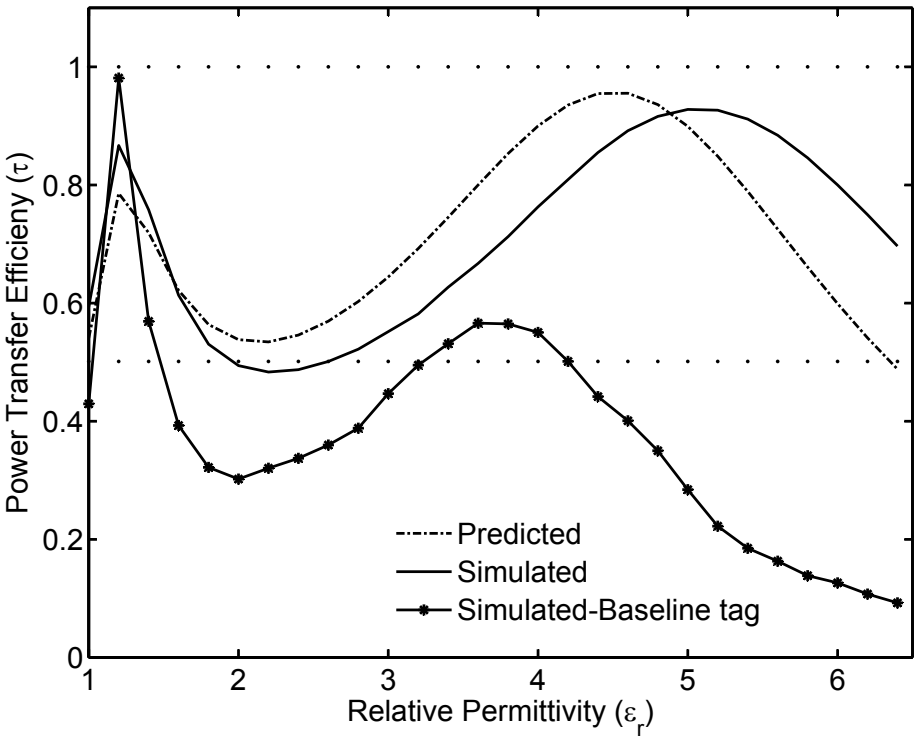

Figure 5.4. Experimental results comparing analytical model and simulation results.

values of ϵ_r, we observe that the baseline tag's efficieny curve looks better than the response of the optimal antenna. But, the performance of the baseline antenna is not sustained as the permittivity increases unlike the optimal antenna. This validates the theoretical approach used to obtain the optimal antenna design.

Chapter 6

Conclusions and Future Work

The passive UHF RFID tags are being extensively used in asset tracking and supply chain management as the tags are easy to fabricate, achieve long read distances and are inexpensive to manufacture. The major drawback of UHF RFID tags is its sensitivity to the environment in which it is used. While the tags have been rigorously evaluated for conductive materials, there has been significantly less rigorous work done on tags in dielectric environments. In this thesis, for the first time, we present a rigorous, theoretical analysis for evaluating RFID tags immersed in dielectric environment using the Uda model of the T-match and embedded-T match antenna. We briefly review the Uda model for T-match and provide equations for Uda parameters like Z_0 and α that are applicable to the planar folded dipole structures. We then propose "immersed Uda model" for a T-match antenna based on the relationship between frequency and immersion in a dielectric medium and validate it using a typical embedded T-match antenna. This model highlights the challenge of operating in a dielectric medium, and the limitations of a high Q antenna.

Using the immersed Uda model, the antenna is first analyzed for optimality

under idealized conditions, namely a perfect impedance match and no change with small perturbations in permittivity. What we discovered is that the optimal Z_0 is not physically realizable with simple printed antennas, and thus the theoretical optimum is impossible to practically realize. Next, we used a brute-force method to find optimal dielectric-bandwidth for a variety of practical scenarios. Also, we propose and validate a more accurate model for common mode impedance Z_c computation to improve the accuracy of the model. The results suggest limits on achievable dielectric-bandwidth and suggest guidelines for designing dielectric-tolerant tags. Finally, we validated the model using a FEM tool. We found that with proper tuning of the antenna design based on the theory, we achieved a robust tag, for a prescribed power transfer efficieny of $\tau_{min} = -3$ dB, works upto maximum possible dielectric constant of 6.4 i.e., it has a impressive *dielectric bandwidth* of 5.4. This result emphasizes the accuaracy of this rigorous model and also highlights the fact that with this theory we can now design robust tag that works well when immersed in a wide range of dielectric media.

We note that there are two important limitations to the approach we present here. First, this work is limited to lossless dielectrics. Second, we consider only immersion in a dielectric medium, which results from a half space case. We suggest that future work consider a reverse transformation from a heterogenous dielectric environment into an equivalent homogeneous dielectric environment. Note that the Uda model suggests that the common and differential modes may have different effective permittivities. Also, since the differential mode consists of coplanar strips, analytical models for layered dielectric media exist and could be applied [12].

We believe that by additional work and alleviating these limitations, we will

be able to achieve a more robust theory and approach for both finding the "best" dielectric-tolerant antenna designs, and providing clear insight into the theory and operation of such antennas in heterogenous environments.

References

[1] Daniel M. Dobkin. *The RF in RFID.* Newnes, 2008.

[2] H. Chaabane, E. Perret, and S. Tedjini. Towards UHF RFID robust design tag. In *2010 IEEE International Conference on RFID*, pages 223 –229, April 2010.

[3] N.A. Mohammed, M. Sivakumar, and D.D. Deavours. An rfid tag capable of free-space and on-metal operation. In *Radio and Wireless Symposium, 2009. RWS '09. IEEE*, pages 63 –66, jan. 2009.

[4] N.A. Mohammed, K.R. Demarest, and D.D. Deavours. Analysis and synthesis of uhf rfid antennas using the embedded t-match. In *2010 IEEE International Conference on RFID*, pages 230 –236, April 2010.

[5] P.V. Nikitin, K.V.S. Rao, S.F. Lam, V. Pillai, R. Martinez, and H. Heinrich. Power reflection coefficient analysis for complex impedances in rfid tag design. *IEEE Transactions on Microwave Theory and Techniques,*, 53(9):2721 – 2725, September 2005.

[6] G. Marrocco. The art of uhf rfid antenna design: impedance-matching and size-reduction techniques. *IEEE Antennas and Propagation Magazine,*, 50(1):66 –79, February 2008.

[7] C.A.Balanis. *Antenna Theory Analysis and Design*. Wliey, New Jersey, 2005.

[8] S.Uda. *Yagi-Uda antenna*. Tohoku University: Research Institute of Electrical Communication, 1954.

[9] R. Lampe. Design formulas for an asymmetric coplanar strip folded dipole. *IEEE Transactions on Antennas and Propagation,*, 33(9):1028 – 1031, sep 1985.

[10] R. Lampe. Correction to "design formulas for an asymmetric coplanar strip folded dipole". *IEEE Transactions on Antennas and Propagation,*, 34(4):611, April 1986.

[11] H.J. Visser. Improved design equations for asymmetric coplanar strip folded dipoles on a dielectric slab. In *The Second European Conference on Antennas and Propagation, 2007. EuCAP 2007.*, pages 1 –6, nov. 2007.

[12] Ramesh Garg et al. *Microstrip antennas design handbook*. Boston, MA : Artech House,, 2001.

[13] J.Galejs. *Antennas in Inhomogeneous Media*. Pergamon Press, New York, 1969.

[14] R.W.P King and G.S.Smith. *Antennas in Matter: Fundamentals, Theory, and Application*. MIT Press, 1981.

[15] D.M. Dobkin and S.M. Weigand. Environmental effects on RFID tag antennas. In *2005 IEEE MTT-S International Microwave Symposium Digest*, page 4 pp., June 2005.

[16] J.D. Griffin, G.D. Durgin, A. Haldi, and B. Kippelen. RF Tag Antenna Performance on Various Materials Using Radio Link Budgets. *IEEE Antennas and Wireless Propagation Letters*, 5(1):247 –250, December 2006.

[17] Y. Amin, Qiang Chen, Botao Shao, J. Hallstedt, H. Tenhunen, and Li-Rong Zheng. Design and analysis of efficient and compact antenna for paper based uhf rfid tags. In *Antennas, Propagation and EM Theory, 2008. ISAPE 2008. 8th International Symposium on*, pages 62 –65, nov. 2008.

[18] Chihyun Cho, Hosung Choo, and I. Park. Design of uhf small passive tag antennas. In *2005 IEEE Antennas and Propagation Society International Symposium*, volume 2B, pages 349 – 352 vol. 2B, July 2005.

[19] T. Deleruyelle, P. Pannier, J. Alarcon, M. Egels, and E. Bergeret. RFID tag antennas with stable impedance to mounted material. In *2010 European Microwave Conference (EuMC)*, pages 1090 –1093, September 2010.

[20] J. Choo, J. Ryoo, and J. Hong. Novel RFID tag antenna with stability to material. In *IEEE Antennas and Propagation Society International Symposium, 2008. AP-S 2008.*, pages 1 –4, July 2008.

[21] G. Manzi and M. Feliziani. Impact of UHF RFID IC impedance on the RFID system performances in presence of dielectric materials. In *2008 International Symposium on Electromagnetic Compatibility - EMC Europe*, pages 1 –6, September 2008.

[22] J. Choo, J. Ryoo, J. Hong, H. Jeon, C. Choi, and Manos M. Tentzeris. T-matching networks for the efficient matching of practical rfid tags. In *Pro-*

ceedings of the 39th European Microwave Conference, pages 5–8, September 2009.

[23] J. David Irwin. *Basic Engineering Circuit Analysis*. MacMillan Publishing Company, New York, third ed. edition, 2005.

[24] M. Hamid and R. Hamid. Equivalent circuit of dipole antenna of arbitrary length. *IEEE Transactions on Antennas and Propagation,*, 45(11):1695 – 1696, nov 1997.